THE FLORIDA STATE UNIVERITY

COLLEGE OF ARTS AND SCIENCES

A PROXY INTEGRATED KINETIC ENERGY FOR TROPICAL CYCLONES IN THE NORTH ATLANTIC

By

SEAN BUCHANAN

A Thesis submitted to the
Department of Earth, Ocean, and Atmospheric Science
to the partial fulfillment of the requirements with
Honors in the Major

Degree Awarded: Spring, 2017.

The members of the Defense Committee approve the thesis of Sean Buchanan defended on November 18, 2016.

Thesis Director: [signature] Date: 11/18/16

2nd Committee Member: [signature] Date: 11/18/16

Outside Committee Member: [signature] Date: 11/18/16

Abstract

The Integrated Kinetic Energy (IKE) of a Tropical Cyclone (TC), a volume integration of the surface winds around the center of the TC is computed from a comprehensive sea surface wind (NASA's Cross-Calibrated Multi-platform [CCMP]) analysis available over the global oceans to verify the fidelity of IKE from wind radii estimates of extended best track (EBT) data maintained by NOAA for the North Atlantic TCs. The years 2004-2011 were examined in this study. It is shown that CCMP surface wind analysis severely underestimates IKE for TCs that are characterized as short in lifespan and small in size. Similarly, large and long lived TCs although reasonably well captured in NASA's CCMP sea surface wind analysis continue to exhibit erroneous areal coverage of the TCs' wind fields that are stronger than gale-force (34-kt; 17 m s^{-1}). The phase of the seasonal cycle of North Atlantic TC IKE also verifies in the CCMP analysis. A proxy IKE (PIKE) based on winds at radius of outermost closed isobar (ROCI) shows greater promise in replicating TC-IKE within the CCMP dataset than the traditional IKE. In other words, PIKE is capable of providing representation of the unresolved traditional TC-IKE values within CCMP that are dependent on wind fields at gale-force and stronger. The diagnosis of PIKE of TCs from CCMP was found to have a linear correlation of 0.8 with corresponding IKE from EBT. This relatively strong correlation raises the possibility of extending past IKE application studies over the northern Atlantic basin to other TC basins using CCMP wind analysis.

1. Introduction

Kantha (2006) initiated the debate to replace the Saffir-Simpson Hurricane Scale (SSHS) – despite its simplistic communication for the general public – after the damage inflicted by tropical cyclones (TCs; e.g., Rita, Katrina, and Wilma) were inaccurately depicted by the SSHS during the 2005 North Atlantic Hurricane Season based on subjective categorization. Kantha (2006) concluded his argument by presenting alternatives to the SSHS with the Hurricane Intensity Index (HII) and Hurricane Hazard Index (HHI), and acknowledged many metrics (including the HII) that communicate risk currently ignore TC wind structure. Following that recognition, Powell and Reinhold (2007) developed a metric known as integrated kinetic energy (IKE) to effectively communicate destructive potential of TCs by emphasizing the importance of TC structure. IKE is the volume integral of the square of the surface winds greater or equal to gale-force winds (34-kt or 17 ms^{-1}) around the eye of a TC (Powell and Reinhold 2007; Misra et al. 2013). Practically IKE is computed as the volume integral of the coverage of the 34-kt, 50-kt and 64-kt winds around the eye of a TC as these wind radii are nominally measured and recorded by the National Hurricane Center (NHC). The integration of kinetic energy has a depth of 1 meter in height making IKE related to the energetics of a TC at the surface. IKE is scaled with both wind load onto structures (ASCE-7 2005) and storm surge and is designed to communicate the destructive potential of a TC and is expressed in units of TeraJoules (TJ; Powell and Reinhold 2007). IKE best represents the impact of storm surge because it is far more sensitive on the wind structure that falls within the critical range of 17 – 33 m s^{-1} (34 – 64-kt; gale-force to hurricane strength); winds that are known to generate stronger storm surge because winds that exceed 33 m s^{-1} have a significant drop off in its drag coefficient causing a weaker stress on the ocean, which is directly related to the strength of the storm surge (Powell et al. 2003; Powell and

Reinhold 2007; Donelan et al. 2004). Since the radial extent of winds weaker than tropical storm strength (17 ms^{-1}) also play an important role in storm surge, it is appropriate to investigate weaker winds found at the TC's radius of the outermost closed isobar (ROCI); a quantity used by Merrill (1984) to describe the areal extent of a TC and subsequently the outer edge of the TC circulation. ROCI is a single valued quantity that averages the cardinal (North, South, East, and West) directional endpoints of the outermost closed isobar (Merrill 1984), and (generally) exceeds that of quadrant data for gale-force winds.

The goals of this research are:

1) To motivate the development of an alternative to existing IKE; validation of TC wind structure fidelity in the best available sea-surface wind analysis
2) To develop the alternative to IKE, which will be called Proxy IKE (PIKE), that will utilize winds found at the outer extent of any given TC circulation (i.e., winds at ROCI).

The appropriate, and immediate response, should be: why do we need a proxy for IKE (PIKE)? To understand this, a brief overview of notable TC-IKE studies will be discussed.

Misra et al. (2013) utilized the concept of IKE by accumulating its total value during a TC's lifespan (track integrated kinetic energy; TIKE) and performed a climate study examining seasonal and interannual variability for TCs in the North Atlantic basin for the years of 1990-2011. In this study, TIKE was compared to ACE (accumulated cyclone energy; Bell et al. 2000), a commonly used metric to measure the seasonal TC activity in a tropical basin. ACE is the square of the maximum sustained winds at every TC observational fix, accumulated over the lifespan of each TC and for all TC's occurring in the season. Yu et al. (2009) and Yu and Chiu's (2012) recognized that ACE's main shortcoming is related to the lack of its emphasis on the

TC's wind structure, which leads to a tendency of overestimating actual variability. Misra et al. (2013) demonstrated that the 2005 Atlantic hurricane season, despite its anomalous feature of having a record number of TCs in a season, was not an anomalous season in terms of TIKE; however, ACE found the 2005 season to be anomalous. This was largely due to a majority of TCs in the 2005 season being characterized as being smaller in size and short lived, resulting in smaller values of TIKE despite a large number of TCs in the season. Misra et al. (2013) also noted that most of the storms in 2005 developed outside the Maximum Development Region (MDR; 10°-20°N, 80°–20°W), which allowed the authors to justify why the 2005 season is indeed not anomalous. Furthermore, the size of the Atlantic Warm Pool (Wang and Enfield 2001) is positively correlated with TIKE, and negatively correlated with sea-surface temperature (SST) variations in the equatorial Pacific hinting at a possible connection to Modoki El Niño (Misra et al. 2013).

Moreover, predicting IKE based on persistence and multivariate normal regression models were found to be potential tools that forecasters could rely on in real time (Kozar and Misra 2014). Statistical Prediction of IKE (SPIKE), used the Atlantic Hurricane Extended Best Track dataset (EBT; Demuth et al. 2006) for the years of 1990-2011 as the training period to develop SPIKE. Then the 2012 season was used as the test interval to serve as a proof of concept for the prediction of IKE using SPIKE. SPIKE was found to explain 80% (60%) of observed variance in IKE for a forecast lead-time of up to 12 (72) hours during the training period for both the training period (1990-2011) and test interval (2012). However, the downfall to IKE prediction is its reliance on TC size parameters that are scarcely available in other tropical ocean basins outside of the North Atlantic basin. In addition, heavy precipitation contaminates remotely

sensed (satellite based) observations and prevents an accurate real-time areal extent of specified wind fields of the TC, which further prevents the utilization of SPIKE.

The aforementioned historical IKE studies, though they have different applications, have one common trait: confinement to the North Atlantic Basin, where specialized aircraft are routinely flown out to gather surface wind measurements (Martin and Gray 1993) and on structural information for TCs dating back to 1988 by the National Oceanic and Atmospheric Administration (NOAA). NOAA recently started gathering similar structural information for TCs that form in the Northeastern Pacific starting in 2001, but this basin has a significantly smaller sample size in comparison to the North Atlantic. In other words, TC-IKE studies have yet to venture outside the tropical North Atlantic Basin. We propose that if a successful alternative to IKE can be developed while capturing and maintaining the integrity of the IKE values, climate scientists and operational meteorologists can enhance risk assessment of TCs for coastal communities while deepening our knowledge on TC variability on a global scale.

The organization for the rest of the paper is as follows. Section 2 will further motivate the need for PIKE by making a case to validate the fidelity of TC fidelity by using the IKE metric in the best-available sea-surface wind analysis provided by National Aeronautics and Space Administration (NASA; Atlas et al. 2011). A brief discussion on the datasets that will be used in the examination of fidelity and in the development of PIKE will be provided, and methodology of validation will be included in the same section. Section 3 will discuss the results of our validation. Sections 4 and 5 will develop motivation for the creation and the results of PIKE respectively. Concluding remarks and discussion will be in the last section.

2. Validation of NASA's Cross-Calibrated Multi-Platform Ocean Surface Wind Vector L3.0 First-Look Analysis

a. Introduction to our Motivation of Validation

Atmospheric and oceanographic reanalysis are major accomplishments achieved by the scientific community that have opened doors of understanding the complexities of climate and its variations over the years. In particular, TC studies have utilized such advancements to understand their structure, dynamics, and influence on climate variability. For instance, using the 40-Year European Centre for Medium-Range Weather Forecasts (ECMWF) Re-Analysis (ERA-40) Hart et al. (2007) studied the local memory of atmospheric and oceanic variability after TC passage; Sriver and Huber (2007) examined the average oceanic heat transport by TCs; influence of TC activity on poleward heat transport through changes to the meridional heat flux (Hart 2010). However, the constant concern of coarse grid resolution and the shortcomings of data assimilation inaccurately representing TCs have always persisted. Many studies have highlighted the limitations of atmospheric reanalysis in representing the intensity and location of the TC's (Schenkel and Hart 2012; Zick and Matyas 2015). Determining the fidelity of the representation of TCs in atmospheric reanalysis was the prime motivation for the works of Schenkel and Hart (2012) who found that the majority of the reanalysis datasets poorly resolve TC location and intensity. LaRow (2013) used the Center for Ocean-Atmospheric Prediction Studies (COAPS) Land-Atmosphere Regional Reanalysis for the Southeast (CLARReS10; Stefanova et al. 2012) at 10km grid interval to study landfalling TCs for the years 1979-2000 and found that near-surface winds were inadequately resolved when compared to observed data. Similarly, Jourdain et al.

(2014) investigated oceanic responses to TC surface winds by extracting wind data from ECMWF operational analysis and ERA-Interim reanalysis. They found that TC surface winds, on average, grossly underestimated intensity parameters causing misrepresentation of vertical mixing and Ekman pumping in the cold wake of the TC passage in the global eddy-permitting ocean reanalyses that were utilized.

Validating the best available sea-surface wind analysis dataset, the National Aeronautics and Space Administration's (NASA's) Cross-Calibrated Multi-Platform Ocean Surface Wind Vector L3.0 First-Look Analysis (hereafter referred to as CCMP; Atlas et al. 2011) for TC application studies is the prime motivation in this section. The purpose of the validating CCMP is to determine if it is a trustworthy dataset that gives a good representation of TC wind fields to apply previous IKE concepts in other tropical ocean basins. Unlike previous studies, we will use the IKE metric to examine the fidelity of TC features in CCMP and will be validated against Extended Best-Track (Demuth et al. 2006) IKE data (the true values of TC-IKE in the North Atlantic) developed by Misra et al. 2013. However, aircraft reconnaissance data is generally unavailable outside the North Atlantic and lacks in temporal continuity. But in fact, aircraft reconnaissance data is available for only 30% of the lifespan of all TCs in the North Atlantic (Rappaport et al. 2009). Landsea and Franklin (2013) even argue that the uncertainty of the best tracked wind data of TCs for the north Atlantic basin are subjectively determined. Nonetheless, Knaff et al. (2016) and Dolling et al. (2016) suggest that the best tracked wind radii are reasonable and provide useful estimates for TC wind structure. Therefore, we are examining the validity of CCMP surface winds for TC-IKE analysis in the tropical North Atlantic Ocean in the hope of extending TC-IKE analysis to other tropical ocean basins accompanied with CCMP.

However, validation has to be done to further motivate and potentially aid in our development of PIKE.

b. Extended Best-Track Aircraft Reconnaissance Data

The Extended Best-Track (EBT) is an extension of the Atlantic Hurricane database (HURDAT) by including structural parameters of a TC per 6-hourly time fix for the years 1988-2014 during its lifetime. The EBT contains operational estimates provided by the National Hurricane Center (NHC) gathered by aircraft reconnaissance (DeMuth et al., 2006). To eliminate errors in operational estimates for EBT, the NHC, starting with the 2004 hurricane season, used postseason reanalysis methods to provide quality estimates of TC structures and started the Best-Track years (2004-present); 1988-2003 are known as the non-Best-Track years in the EBT. Notable features of the EBT is its informative detail on 34-, 50-, and 64-kt radii for primary intercardinal (Northwest, Northeast, Southwest, and Southeast) directional quadrants, radius of maximum winds (RMW), pressure and radius of the outermost closed isobar (POCI and ROCI respectively), minimum sea-level pressure (MSLP), maximum 1-minute sustained winds (VMAX), latitude and longitude positioning of TC center, eye diameter, distance to nearest landmass, and storm classification. The EBT has been historically used in previous IKE studies (Misra et al 2013; Kozar and Misra 2014; refer back to section 1 for more details). A historic IKE dataset was created for the years of 1990-2011 in Misra et al. (2013). The first two years in the EBT (1988-89) were excluded in Misra et al. (2013) due to its incomplete coverage. IKE for the years 2012-2014 are added to the historic dataset. By doing so, this provides a larger sampling size covering two out of the three temporal categorizations in EBT (1990-2014; 2004-2014).

c. CCMP Winds

The CCMP analysis provides sea-surface winds at a height of 10 meters around the globe apart from the Arctic Ocean (Atlas et al. 2011). It has been widely used for several ocean related studies (Zheng et al. 2016; Oey et al. 2013) including TC studies (Zhang et al. 2013; Vukicevic et al. 2014; Pei et al. 2015). The CCMP surface wind analysis is available at 0.25° grid spacing at 6-hourly intervals with the same 6-hourly temporal resolution found in EBT from 1987-2011. This analysis has been developed using the Variational Analysis Method (VAM) that combines in situ, remotely sensed observations (microwave radiometers and scatterometers; e.g., WindSat and QuikScat respectively), and first guess estimate from analyses (from 1987-1998 ECMWF reanalysis [ERA-40] was used, and ECMWF operational analysis thereafter). In situ observations (e.g., moored buoys) over the ocean are known to be sparse, therefore; data from polar orbiting satellites make up the bulk of the CCMP wind product. Polar orbiting satellites are known for excluding wide areas near and at the equator. In order to ameliorate the aforementioned problem, the inclusion of Tropical Rainfall Measuring Mission Microwave Imager (TMI) provides complete coverage of the tropics (30°S to 30°N) and augments the analysis of the sea-surface winds in CCMP.

d. Methodology of Validation

The definition of IKE provided by Powell and Reinhold (2007) is:

$$IKE = \frac{1}{2}\int_V \rho U^2 dV \qquad (1)$$

Where ρ is a constant value for air density which is taken to be 1.15 kg m^{-3}. U is the surface wind speed and the integration is a volume integral of the surface winds for a thickness of 1 meter. The historical North Atlantic TC IKE dataset created by Misra et al. (2013) will be used as the validation dataset when comparing the fidelity of contemporaneous TC-IKE values found in CCMP. It is well known that the size of the TC has a stronger bearing on IKE than the peak wind speeds (Reinhold and Powell 2007; Musgrave et al. 2012; Kozar and Misra 2014). Therefore, the size (or spatial extent) of the 34-kt winds for TCs play a significant role in the total IKE than the comparatively smaller spatial extent of the 50-kt and 64-kt winds (Kozar and Misra 2014).

To determine the fidelity of TC-IKE in CCMP, we examined the total IKE for all wind speeds greater than or equal to 34-kt winds. Afterwards, the IKE for winds greater than or equal to 50- and 64-kt winds were separately considered. The purpose of breaking IKE into different piecewise components is to help determine the percentage of resolved wind fields within the dataset. To distinguish the difference between these three IKE quantities in CCMP validation they have been assigned to the following names: Total CCMP IKE (TCI) represents IKE for U ≥ 34-kts; 50-kt IKE represents IKE only for U ≥ 50-kts; 64-kt IKE represents IKE only for U ≥ 64-kts. A similar process was done with the EBT TC-IKE by including and excluding specified wind fields.

It should be noted that the EBT considers the asymmetries in the surface wind structure of the TC by providing estimates of wind radii in the primary intercardinal directional quadrants (Northeast, Southeast, Southwest and Northwest) of the TC at each 6-hourly time fix. However, CCMP being a gridded analysis provides an opportunity to examine an accurate account of TC surface wind asymmetries.

We found that CCMP poorly resolves IKE starting at wind speeds of 50-kt and 64-kt winds (and stronger) in TCs of the tropical North Atlantic. In fact, of the 1497 (942) fixes of TCs that had 50-kt (64-kt) winds in the EBT data (for the period 2004-2011) there were only 220 (45) resolved fixes, which does not consider accuracy in the corresponding CCMP analysis respectively. In other words, 14.7% (4.8 %) fixes were resolved in CCMP for IKE with $U \geq 50$-kt (64-kt) with EBT. Therefore, in discussing the results we have limited our analysis to examining TCI.

Table 1 shows that the 34-kt radii variation explains more variance than the radii of the other two specified wind regimes in the EBT data. Furthermore, the choice of using median, average or root mean squared value of the wind radii in the four quadrants of the TC had insignificant bearing on the variance of IKE in the EBT dataset (Table 1). This suggests that the asymmetries in the surface wind of the TC resolved by EBT are relatively small. It may be noted that Table 1 also suggests that these conclusions remain consistent both in years prior and in the best tracked years of the EBT dataset.

3. CCMP Validation Results

The EBT dataset contains 2353 6-hourly time fixes of TCs with 34-kt piecewise IKE (which is $IKE_{18\text{-}26}$ in appendix of Misra et al. 2013) values for the years 2004-2011. However, CCMP only resolved 1090 (46.4%) out of the aforementioned 6-hourly time fixes. Atlas et al. (2011) clearly indicate that all microwave sensors used in the CCMP analysis are sensitive to rain with increasing rain rate associated with decreased accuracy and data gaps of satellite retrieved winds. A scatter plot between resolved TCI against EBT's $IKE_{18\text{-}26}$ (Fig. 1a) and total

(Fig. 1b) IKE showcases the fidelity of the CCMP winds. It may be noted that Kozar and Misra (2014) found that the areal extent of the 34-kt wind fields plays a vital role in the variance of IKE than the other two relatively smaller wind fields of 50- and 64-kt, consistent with the correlations shown in Table 1.The explained variance of EBT's $IKE_{18\text{-}26}$ to TCI (R^2 = 57%) in Fig. 1a is less than that of the TCI and total IKE from EBT (R^2=71%; Fig. 1b). The difference in the R^2 value between Figs. 1a and b suggest that TCI is capable of explaining approximately 70% of the variability of total IKE in EBT, and it suggests that there is minimal resolution in the extent of the actual 34-kt wind field in CCMP (Fig. 1a; R^2=57%). Fig. 1a also suggests that there is a systematic underestimation in the size of winds greater than or equal to 34-kt winds in CCMP relative to EBT's $IKE_{18\text{-}26}$. In fact, the relatively higher R^2 value in Fig. 1b suggests that in some of the more intense TCs, the spatial extent of the 34-kt wind is overestimated in CCMP and compensates for the underestimation of the higher wind speeds relative to EBT data. Similarly, Fig. 1b also shows that Total IKE from CCMP underestimates the total IKE from EBT. The larger RMSE values in Fig. 1b compared to Fig. 1a reinforce the aforementioned points.

In comparing Figures 2 and 3 it is clear that CCMP has difficulty in resolving TCs that are at the extreme ends of size, lifespan, and $IKE_{18\text{-}26}$ values (Figs. 2b and 3b). But the bias for smaller sized, short lived TCs in the CCMP analysis is quite apparent. CCMP detected 86 TCs, with wind speeds at 34-kt winds and greater compared to EBT's 129 for the 2004-2011 time period of study. Smaller sized TCs tend to have smaller values in IKE because of IKE's reliant nature on the size of the TC. The relatively coarse grid resolution and limitations of the data (e.g. coverage), first guess field used in the analysis is the probable explanation as to why smaller TCs', gale-force winds are not being detected in CCMP. Large TCs with a long lifespan found in

the open ocean (and more frequently west of 60W; Figs. 2b and 3b are, for the most part, resolved in its entirety in the CCMP analysis. However, these large TCs in the open ocean in the CCMP wind analysis are grossly underestimated in its areal extent of the wind regime characterized by gale-force winds giving rise to their underestimation in the CCMP analysis.

The climatological seasonal cycle (CSC) of TC-IKE and number of TCs computed over the period of 2004-2011 are shown in Fig. 4. Fig. 4a indicates that IKE and number of storms peak in the month of September in the EBT dataset, which is consistent with earlier studies (Gray 1968;Misra et al. 2013). The corresponding CSC for CCMP analysis (Fig. 4b) appears to display the same distribution to that of EBT's (Fig. 4 a). However, comparing Figs. 4a and b, the systematic underestimation of IKE and the number of TC's resolved in CCMP is apparent.

We also computed the track density expressed as the number of TCs with at least 34-kt winds per 1°x1° cell from both EBT and CCMP analysis (Fig. 5). It may be noted that TCs that stayed within one cell for multiple 6-hourly time fixes were not counted more than once in preparing Fig. 5. In comparing Figs. 5a and b a number of features can be noted: i) The overall track density across North Atlantic Ocean is generally less in CCMP relative to EBT and ii) the gross characteristics of these tropical storm strength TCs like their recurvature in the higher latitude ocean, higher density of TCs west of 60°W are reasonably well captured in CCMP analysis. There could be several reasons for this. Foremost being that TC fixes over the open oceans in eastern Atlantic are likely to be genesis or near genesis locations, which would make them comparatively smaller in size than those that have traversed to the western Atlantic Ocean over a period of time. Furthermore, there is far more incidence of TC fixes in the open ocean in the EBT data than near the coasts. Another reason is that in the open ocean there is an over reliance on remotely sensed wind that is contaminated by rain clouds of the TC and results in

less coverage as compared to near shore TCs that are more likely to be resolved in the background reanalysis field owing to alternative observations (Atlas et al. 2011). In a related study, Kimball and Mulekar (2004) conducted a climatological analysis of the EBT data and found that TCs in the Gulf of Mexico have larger radii of outermost closed isobar while exhibiting a smaller radial extent of 34-, 50-, and 64-kt winds compared to TCs found in 50°−80°W, which may explain the comparatively low track density observed over the Gulf of Mexico in the CCMP winds. All in all, the evidence of poor TC fidelity in the North Atlantic basin within the best available sea-surface wind analyses provides irrefutable need for a proxy to exploit the verification of the actual value of TC-IKE.

4. Motivational Development of PIKE

a. Motivational Development of PIKE

Here we will exploit the definition of IKE (refer to Equ. 1; Powell and Reinhold 2007) to develop an appropriate proxy for IKE (PIKE) that only considers information of ROCI. We define PIKE as the volume integral of the winds at ROCI. The essential ingredients of PIKE are: ROCI (prescribes the areal coverage in the volume integration), and winds at ROCI. The caveats to PIKE: ROCI is a single quantity (based on EBT) that obviously ignores the asymmetries of the TC; furthermore, there is no available data on the wind intensities found at ROCI from EBT and therefore we have to rely on alternative sources. We obtain PIKE in a number of different ways including the use of theoretical mass-wind relations and the use of empirical TC wind structure.

Two theoretical mass-wind relations – Gradient wind balance (Equ. 2) and cyclostrophic balance (Equ. 3) – are used to derive winds at ROCI obtained from EBT.

$$V_{gr} = -\frac{fr}{2} \pm \sqrt{\frac{f^2r^2}{4} + \frac{1}{\rho}\frac{\partial p}{\partial lnr}} \quad (2)$$

$$V_{cyclo} = \pm\sqrt{\frac{1}{\rho}\frac{\partial p}{\partial lnr}} \quad (3)$$

The positive roots in the above two equations ($V_{cyclo/gr} > 0$; indicates cyclonic flow) were taken to be U in Equ. 1 when developing our motivation for PIKE. Typical TC wind modeling commonly use Pure and Modified Rankine Vortex with the latter using a scale parameter. Rankine Vortex is a piecewise function that models the circulation's winds as linearly increasing from the center to RMW, and decays thereafter. Since we are only interested in the outer wind profile, we will only utilize the portion of the Rankine Vortex that describes the outward decay,

$$V(r) = VMAX(\frac{RMW}{r})^A \quad (4)$$

where A is the decay parameter, which was set at 0.5 for the modified version that considers frictional dissipation in the flow. Conversely, the decay parameter was set to equal 1.0 for the pure form. The variable r is set to equal the ROCI value. For each motivational development case, the volume integration became $\pi H(ROCI)^2$, where H = 1 m in height and π is the mathematical ratio (constant) of a circle's circumference to its diameter. To avoid any confusion, the term pseudo-PIKE will be given to these motivational models.

b. Practical development of PIKE: Extracting Winds at ROCI from CCMP using EBT data

ROCI is provided as a single valued quantity (in unit nautical miles; nm) in EBT, which reinforces the claim that this parameter is poorly documented with no estimates of uncertainty or asymmetries thereof (Knaff et al. 2014). In other words, we have no quadrant data for ROCI unlike 34-, 50-, and 64-kt winds, and are forced to assume solid body rotation (hence, why the

volume integration becomes the volume of a cylinder $\pi H(ROCI)^2$). However, from Merrill (1984), we know that ROCI is an averaged quantity of the cardinal directional endpoints (North, South, East and West) of the outermost closed isobar with specified constraints depending where the TC is at in its lifecycle. Therefore, information on the position of the center of the TC and ROCI provided by EBT will be used to extract winds found at ROCI when using CCMP.

In the previous section, we demonstrated the poor fidelity of TC-IKE representation for winds at an intensity of 34-kt or greater, but we have no concern that the values being extracted are contaminated due to heavy precipitation because ROCI, generally speaking, greatly exceeds that of the radial extent of gale-force winds, which means we expect weaker winds which are associated with minimal deep atmospheric convection. There are instances in the EBT where ROCI is smaller than the spatial extent of gale-force winds, which implies that asymmetries of the TC will influence some results; EBT data suggest that this only occurs when the TC enters extra-tropical transition and resides in the midlatitudes.

ROCI is converted from nautical miles to the nearest whole degree (1 nm = 1.852 km; 1° = 111.111 km). Starting at the center position of the TC, the magnitude of the winds at the cardinal directional endpoints with a distance of ROCI (in nearest whole degree) will be extracted and averaged and will be used as the value of U when plugged into Equ. 1 (IKE).

5. PIKE Results

Theoretical wind-mass relations (cyclostrophic and gradient wind balance) and Pure and Modified Rankine Vortexes (hereafter referred to as PRV and MRV respectively) are used to simulate a possible wind field found at ROCI and plugged in for as U into IKE (Equ. 1) after

volume integration of ROCI. Poor correlations were generated between EBT IKE and the pseudo-PIKEs that incorporates gradient wind balance and PRV for U in Equ.1 (Table 3). Conversely, higher correlations for the pseudo-PIKE that sets U to equal the MRV and cyclostrophic wind balance for the Best-Track temporal category (2004-2014) in the EBT (Table 3); in fact, higher correlations were found in all three temporal categories of the EBT in comparison. This suggests that the flow at ROCI is more likely to be cyclostrophic than a flow in gradient wind balance. Furthermore, the linear correlations found in Table 2 tells us that ROCI has a stronger bearing on IKE than two parameters that are already used in IKE (RMW and VMAX; Appendix in Misra et al. 2013). It's apparent, from theoretical wind profiles, solid body assumptions of ROCI, and examination of TC structural parameters, that the development of PIKE utilizing information of ROCI has merit.

For the years 2004-2011, EBT IKE and PIKE has a linear correlation of 0.8040 (Fig. 6a; Table 4). Even though this is a similar linear correlation to resolved TCI in the previous section (R=0.8403; Fig. 1b; Table 4) there are notable differences. For instance, PIKE has a larger sample size (2353 6-hourly time fixes and as may in EBT) than TCI (1090 6-hourly time fixes) with a minimal discrepancy between RMSE. This indicates that the discrepancies are not statistically significant, but the flipside of PIKE is that it is able to exploit the verification of IKE within CCMP that could not be observed directly through the regular definition of IKE with $U \geq$ 34-kt. Moreover, for the years of study the linear correlation between EBT IKE and PIKE varies from ~0.6 to ~0.9; the same is said for the resolved TCI fixes (Table 4).

It is widely known that the ROCI parameter is poorly documented and processed subjectively (Knaff et al. 2014). However, our results provide a rough approximation of the intensity for the winds at ROCI based on solid-body assumptions provided by EBT in the CCMP

extraction. For the years 2004-2011, a climatological average for the interquartile range, i.e., 25th – 75th percentile, gives the intensity of ROCI a range of 7.8 – 10.7 m s^{-1} with a median averaged quantity of 9.2 m s^{-1} (Table 5). The minimum average intensity for ROCI is around 3.7 m s^{-1}, while the maximum average intensity is 16.5 m s^{-1}. The minimum averaged value corresponds to smaller TCs in the early stages of its lifespan. Upon looking at Table 5, it is apparent that a few of the maximum intensities for ROCI are at or above gale-force strength (17 m s^{-1}), which is primarily due to TCs that have undergone extra-tropical transition where asymmetric features become commonplace in the structure of the TC (Kimball and Mulekar 2004; Evans and Hart 2003). Consequently, solid-body assumptions of ROCI have failed within the EBT dataset because it highlights the aforementioned problem in Section 1 that the radial extent of 34-kt winds exceed ROCI.

The results of the intensity extracted for ROCI from CCMP suggest that the magnitude of the wind speed is relevant. The concern that the flow at ROCI may be mingling with the outside environmental flow, based on the magnitude of the flow from within the interquartile range (Table 5), should only be considered for TCs in their early stages of genesis.

A composite track density for the TC time fixes for which PIKE validates most poorly (Fig. 8a) and closely (Fig. 8b) indicates the precision of PIKE. The 10th and 90th percentile of absolute difference between IKE and PIKE (|IKE – PIKE|) where taken to be the cutoff marks for the 6-hourly time-fixes that validate the most closely and poorly respectively. The value for the 10th (90th) percentile in absolute difference is 0.9227 TJ (55.6737 TJ). It is quite apparent that PIKE poorly validates with EBT IKE once the TC undergoes extra-tropical transition, which can be seen through recurvature in the midlatitudes north of 24°N, and where in situ observations are more likely to be sparse east of 60°W in the open ocean, which is known to influence the quality

of CCMP winds (Atlas et al. 2011). Conversely, PIKE performs excellently for TCs close to land, specifically, south of 24°N and west of 60°W.

6. Conclusion

a. Validation of CCMP TC-IKE fidelity.

In this paper, we examine the fidelity of the TC-IKE over several hurricane seasons (2004-2011) of the North Atlantic in the Cross-Calibrated Multi-Platform Ocean Surface Wind Vector L3.0 First-Look (CCMP) analysis to motivate the need of a proxy IKE (PIKE). We used the Extended Best Track (EBT; Demuth et al. 2006) IKE dataset (Misra et al. 2013) for validation. IKE relies on the structure of specified surface wind regimes, which makes it a reliable metric to estimate potential damage from storm surge and wind load on structures. Because IKE is not dependent on a transient feature like the peak sustained wind speed but volume integrates the surface wind from the center of the TC out to 34-kt wind speed, i.e., U ≥ 34-kt (17 m s^{-1}), it has considerable inertia and therefore has the potential to be simulated or predicted better than other TC metrics (Kozar and Misra 2014). The CCMP analysis was found to barely resolve the wind fields greater than or equal to 50-kt (26 m s^{-1}) and 64-kt (33 m s^{-1}) winds. It also became apparent that CCMP grossly misrepresents the 34-kt wind field in the majority of TCs.

We therefore computed Total CCMP IKE (TCI; U ≥17 m s^{-1}), which was found to explain approximately 70% of the variance of total IKE in the EBT data. However, only ~46% of the observed 6-hourly fixes in EBT were resolved from EBT most of which were grossly misrepresented. We then validated the TCI analysis by comparing it to EBT's $IKE_{18\text{-}26}$ to get a

clear picture of the 34-kt wind field, which is known to have a strong bearing on IKE (Kozar and Misra 2014). It was found that CCMP poorly resolved the areal extent of gale-force (34-kt; 17 m s^{-1}) strength winds for TCs that are small in size with a short lifespan reinforcing our previous claim. Large TCs with long lifespans are invariably resolved irrespective of their location (either in the open ocean or near the coast). However, the areal coverage of gale-force winds for large TCs are also underestimated in the CCMP analysis relative to EBT dataset.

Qualitatively, the climatological seasonal cycle of total IKE and their number of fixes in the North Atlantic are reasonably well captured by the CCMP winds. However, quantitatively they grossly underestimate IKE and the number of fixes relative to EBT data.

The track densities for the resolved fixes of TCI reveal much lighter density across the North Atlantic basin compared to EBT's complete coverage of total IKE data. The differences in the track densities are far more apparent in the open ocean than near the coasts. TCs in the Gulf of Mexico, south of the main islands in the Caribbean and north of the South American Coast are also poorly resolved. CCMP's poor resolution of TCs as depicted by its IKE values for TCs in the tropical North Atlantic can best be described by lack of in situ observations in the open ocean, contamination of remotely sensed winds due to heavy precipitation, and (potentially) the spatial resolution of CCMP is still coarse enough to not resolve TC gale-force strength winds (and higher) properly.

b. PIKE

The gross misrepresentation and underrepresentation of TC wind fields in CCMP provides a clear need for a proxy IKE (PIKE) to help exploit missing IKE data. PIKE utilizes

structural and wind intensity information on the radius of the outermost closed isobar (ROCI). There were immediate problems with ROCI because of its poor and subjective documentation (Knaff et al. 2014); ROCI is a single averaged quantity (Merrill 1984) and there is no wind data that coincides with the 6-hourly ROCI data provided by EBT. Therefore, motivational pseudo-PIKEs were developed using ROCI (solid body rotation) with theoretical mass-wind relations and typical TC wind modeling outside the radius of maximum winds. The pseudo-PIKEs confirmed that solid-body rotation is a good foundation for volume integration. Pseudo-PIKEs also suggest that the intensity is cyclonic in nature (i.e., minimal entrainment form the environmental anticyclonic flow), and keeping it constant throughout the areal coverage of the solid-body TC, based on ROCI, is also a good approximation.

Despite the promising results of the pseudo-PIKEs, which served as a proof of concept, the actual value for the magnitude of the winds found at ROCI were still needed. ROCI wind extraction utilized contemporaneous EBT and CCMP data. As mentioned earlier, CCMP poorly represents the 34-, 50-, and 64-kt wind fields that make up the structure of any given TC. However, we assume that CCMP properly resolves the wind intensity beyond the radial extent of 34-kt out toward ROCI where less intense deep atmospheric convection can contaminate remotely sensed observations. PIKE was found to have similar climatological correlation for the years 2004-2011 with EBT IKE to Total CCMP IKE (TCI) of ~0.8. The main difference between the two correlations is a dramatic difference in sample size; PIKE had a larger sample size than TCI. For the entire temporal study (2004-2011), PIKE varied in correlation from ~0.6 to ~0.9.

The distribution of the magnitude of the winds found at ROCI – after EBT/CCMP extraction – can be visualized with the usage of boxplots. The averaged interquartile range intensities for ROCI are found to be between 7.8 – 10.7 m s^{-1} (Table 5). The median averaged

quantity was 9.2 m s^{-1}. Maximum values that exceed or come close to gale-force strength (34-kt) are due to asymmetrical features of the TC and poorly estimated radial values for ROCI after the TC underwent extra-tropical transition. We would like to stress that the intensities found at ROCI through an extraction process (refer to Section 4) are not the true values of the ROCI intensity because the extraction process was limited to poorly documented data.

A composite track density of where PIKE does the best and poorly based on the 10^{th} and 90^{th} percentile of the absolute difference between PIKE and EBT IKE respectively. The cutoff mark of the 10^{th} (90^{th}) percentile is 0.9227 (55.6737) TJ. PIKE is found to do well for TCs south of 24°N and west of 60°W, and poorly north of 24°N and east of 60°W where TCs typically recurve in the open ocean, which is characterized with dearth in situ data.

Currently, there are many operational setbacks with remotely sensing TC wind fields with attempts to improve them (Demuth et al. 2004; Knaff et al. 2016), and IKE has been demonstrated to be useful if it's in the arsenal of forecasters and risk management (Kozar and Misra 2014; Powell and Reinhold 2007). Our hope is to have PIKE utilized by forecasters and research scientists alike in all major ocean basins. The usage of winds at ROCI and not the other wind fields will be advantageous since remotely sensed observations are less likely to be contaminated by heavy amounts of precipitation. Moreover, PIKE has the potential of opening our eyes to a global perspective of TC variability as well as saving lives. We realize that our results on the intensity of ROCI is not the exact truth, but they do indicate relevance to the structure of a TC and needs a thorough investigation.

7. References

ACSE, 2005: ASCE 7-05: Minimum design loads for buildings and other structures. American Society of Civil Engineers, 424 pp.

Atlas, R., R. N. Hoffman, J. Ardizzone, S. M. Leidner, J. C. Jusem, D. K. Smith, D. Gombos, 2011: A cross-calibrated, multiplatform ocean surface wind velocity product for meteorological and oceanographic applications. *Bull. Amer. Meteor. Soc.*, **92**, 157-174, doi: 10.1175/2010BAMS2946.1.

Bell, G. D., and Coauthors, 2000: Climate assessment for 1999. *Bull. Amer. Meteor. Soc.,* **81**, S1–S50.

Demuth, J. L., M. DeMaria, J. A. Knaff, and T. H. Vonder Haar, 2004: Evaluation of advanced microwave sounding unit tropical-cyclone intensity and size estimation algorithms. *J. Appl. Meteor.*, **43**, 282-296.

Demuth, J., M. DeMaria, and J.A. Knaff, 2006: Improvement of advanced microwave sounder unit tropical cyclone intensity and size estimation algorithms. *J. Appl. Meteor.*, **45**, 1573-1581.

Dolling, K., E. A. Ritchie, and J. S. Tyo, 2016: The use of the deviation angle variance technique on geostationary satellite imagery to estimate tropical cyclone size parameters. *Wea and Forecasting*, doi: http://dx.doi.org/10.1175/WAF-D-16-0056.1. In press.

Evans, J. L., and R. E. Hart, 2003: Objective indicators of the life cycle evolution of extratropical transition for atlantic tropical cyclones. *Mon. Wea. Rev.*, **131**, 909-925.

Gray, W. M., 1968: Global view of the origins of tropical disturbances and storms. *Mon. Wea. Rev.*, **96**, 669–700.

Hart, R.E., 2010: An inverse relationship between aggregate tropical cyclone activity and subsequent winter climate. *Geo. Res. Lett.*, **38**, L01705, doi:10.1029/2010GL045612.

Hart, R., R. Maue, and M. Watson, 2007: Estimating the atmospheric and SST memory of tropical cyclones through MPI anomaly evolution. *Mon. Wea. Rev.*, **135**, 3990-4005.

Jourdain, N. C., B. Barnier, N. Ferry, J. Vialard, C. E. Menkes, M. Lengaigne, and L. Parent, 2014: Tropical cyclones in two atmospheric (re)analyses and their response in two oceanic reanalyses. *Ocean Modelling,* **73**, 108-122.

Kimball, S., and M. Mulekar, 2004: A 15-Year Climatology of North Atlantic Tropical Cyclones, Part 1: Size Parameters. *Journal of Climate*, **17**, 3555-3575.

Knaff, J. A., S. P. Longmore, D. A., Molenar, 2014: An objective satellite-based tropical cyclone size climatology. *Journal of Climate*, **27**, 455-476.

Knaff, J. A., C. J. Slocum, K. D. Musgrave, C. R. Sampson, B. R. Strahl, 2016: Using routinely available information to estimate tropical cyclone wind structure. *Mon. Wea. Rev.*, **144**, 1233-1247.

Kozar, M. E., and V. Misra, 2014: Statistical Prediction of Integrated Kinetic Energy in North Atlantic Tropical Cyclones. *Monthly Weather Review*, **142**, 4646-4657.

Landsea, C. W. and J. L. Franklin, 2013: Atlantic hurricane database uncertainty and presentation of a new database format. Mon. Wea. Rev., 141, 3576-3592.

LaRow, T., 2013: An analysis of tropical cyclones impacting the Southeast United States from a regional reanalysis. *Regional Environmental Change* **13:S1**, 35-43.

Martin, J. D., and W. M. Gray, 1993: Tropical cyclone observation with and without aircraft reconnaissance. *Wea. and Forecasting*, **8**, 519-532.

Misra V., S. DiNapoli, and M. Powell, 2013: The Track Integrated Kinetic Energy of Atlantic 615 Tropical Cyclones. *Monthly Weather Review* **141**:7, 2383-2389.

Musgrave K.D., R. K.Taft, J. L.Vigh, B. D.McNoldy, *and* W. H.Schubert, 2012: Time evolution of the intensity and size of tropical cyclones, J. *Adv. Model. Earth Syst.,* **4**, M08001.

Oey, L. –Y., M.-C. Chang, Y.-L. Chang, Y.-C. Lin, F.-H. Xu. (2013) Decadal warming of coastal China Seas and coupling with winter monsoon and currents. *Geophysical Research Letters* **40**:23, 6288-6292.

Pei, Y.H., RongHua Zhang, DaKe Chen. (2015) Upper ocean response to tropical cyclone wind forcing: A case study of typhoon Rammasun (2008). *Science China Earth Sciences* **58**:9, 1623-1632.

Powell, M.D., and T.A. Reinhold, 2007: Tropical Cyclone Destructive Potential by Integrated 627 Kinetic Energy. *Bull. Amer. Meteor. Soc.*, **88**, 513–526.

Rappaport, E. N., and Coauthors, 2009: Advances and challenges at the National Hurricane Center. *Wea. Forecasting*, **24**, 395–419, doi:10.1175/2008WAF2222128.1.

Schenkel, B. and R. E. Hart, 2012: An examination of tropical cyclone position and intensity differences within reanalysis datasets. *J. Climate*, MERRA Special Collection, **25**, 3453-3475. doi: 10.1175/2011JCLI4208.1.

Sriver, R., and M. Huber, 2007: Observational evidence for an ocean heat pump induced by tropical cyclones. *Nature*, **447**, 577–580.

Stefanova, L., V. Misra, S. Chan, M. Griffin, J. O'Brien, and T. Smith, 2012: A proxy for high-resolution regional reanalysis for the Southeast United States: assessment of precipitation variability in dynamically downscaled reanalysis. *Clim Dyn.,* **38**:2449–2466.

Uppala, S., and Coauthors, 2005: The ERA-40 Re-Analysis. *Quart. J. Roy. Meteor. Soc*., **131**, 2961–3012.

Vukicevic, T., Eric Uhlhorn, Paul Reasor, Bradley Klotz. (2014) A Novel Multiscale Intensity Metric for Evaluation of Tropical Cyclone Intensity Forecasts. *Journal of the Atmospheric Sciences* **71**:4, 1292-1304.

Wang, C., and D. B. Enfield, 2001: The tropical western hemisphere warm pool. *Geophys. Res. Lett*., **28**, 1635-1638.

Yu, J.-Y., and P.-G. Chiu, 2012: Contrasting various metrics for measuring tropical cyclone activity. *Terr. Atmos. Oceanic Sci.*, **23**, 303–316.

Yu, J. –Y., C. Chou, and P.-G. Chiu, 2009: A revised accumulated cyclone energy index. *Geophys. Res. Lett.*, **36**, L14710, doi:10.1029/2009GL039254.

Zhang, R. –H., Yuhua Pei, Dake Chen. (2013) Remote effects of tropical cyclone wind forcing over the western Pacific on the eastern equatorial ocean. *Advances in Atmospheric Sciences* **30**:6, 1507-1525.

Zheng, C. W., Jing Pan, Chong Yin Li. (2016) Global oceanic wind speed trends. *Ocean & Coastal Management* **129**, 15-24.

Zick, S. E., C. J. Matyas, 2015: Tropical cyclones in the North American Regional Reanalysis: An assessment of spatial biases in location, intensity, and structure. *Journal of Geophysical Research: Atmospheres* **120:5**, 1651-1669.

Table 1: The correlation of Integrated Kinetic Energy (IKE) with wind radii from Extended Best Track (EBT) data (Demuth et al. 2006) for three different time periods and three different estimates of radii (mean, median, and root mean squared) measured at the 4 quadrants of a TC. Best-Track years are characterized by quality-controlled values. 95% confidence intervals for the correlation coefficient are included in parentheses.

Correlation table of wind radii distributions versus IKE			
Median wind radii measurements			
	All years (1990-2014)	Non-Best-Track years (1990-2003)	Best-Track years (2004-2014)
34-kt radii	0.8919 (0.8863 to 0.8966)	0.8905 (0.8827 to 0.8972)	0.9014 (0.8941 to 0.9076)
50-kt radii	0.8171 (0.8082 to 0.8248)	0.8109 (0.7981 to 0.8221)	0.8189 (0.8063 to 0.8299)
64-kt radii	0.6744 (0.6600 to 0.6873)	0.6452 (0.6238 to 0.6647)	0.7065 (0.6876 to 0.7235)
Averaged wind radii measurements			
34-kt radii	0.9148 (0.9103 to 0.9185)	0.9236 (0.9180 to 0.9283)	0.9284 (0.9230 to 0.9329)
50-kt radii	0.8298 (0.8214 to 0.8370)	0.8378 (0.8266 to 0.8475)	0.8264 (0.8143 to 0.8370)
64-kt radii	0.6837 (0.6696 to 0.6963)	0.6486 (0.6274 to 0.6679)	0.7263 (0.7085 to 0.7423)
Root Mean Squared wind radii			
34-kt radii	0.9212 (0.9170 to 0.9246)	0.9092 (0.9026 to 0.9148)	0.9240 (0.9183 to 0.9288)
50-kt radii	0.8351 (0.8270 to 0.8421)	0.8280 (0.8162 to 0.8383)	0.8259 (0.8138 to 0.8365)
64-kt radii	0.6941 (0.6804 to 0.7063)	0.6485 (0.6273 to 0.6678)	0.7527 (0.7363 to 0.7673)

Table 2: The correlations of IKE with radii of specified winds and maximum sustained wind speed (VMAX) from Extended Best-Track (EBT; Demuth et al. 2006). RMW and ROCI are radius of maximum wind speed and radius of the outermost closed isobar of the TC respectively. The average radii of the 34-, 50-, and 64-kt winds are over the 4 quadrants of the TC. 95% confidence intervals are included in parentheses.

Correlation Table versus IKE			
	All years (1990-2014)	Non-Best-Track years (1990-2003)	Best-Track years (2004-2014)
Average 34-kt radii	0.9148 (0.9103 to 0.9185)	0.9092 (0.9026 to 0.9148)	0.9284 (0.9230 to 0.9329)
Average 50-kt radii	0.8289 (0.8205 to 0.8362)	0.8280 (0.8162 to 0.8383)	0.8264 (0.8143 to 0.8370)
Average 64-kt radii	0.6837 (0.6696 to 0.6963)	0.6485 (0.6273 to 0.6678)	0.7263 (0.7085 to 0.7423)
RMW	0.0523 (0.0273 to 0.0771)	0.0188 (-0.0162 to 0.0537)	0.0523 (0.0165 to 0.0878)
ROCI	0.5642 (0.5464 to 0.5805)	0.5655 (0.5407 to 0.5883)	0.6052 (0.5815 to 0.6269)
VMAX	0.4527 (0.4322 to 0.4719)	0.4538 (0.4251 to 0.4807)	0.4501 (0.4207 to 0.4777)

Table 3: The correlations between IKE and a variety of theoretical mass-wind relations designed to motivate PIKE for winds found at ROCI (see text). 95% confidence intervals are included in parentheses.

Correlation Table Between Proxies and IKE			
Vs. IKE	All years (1990-2014)	Non-Best-Track Years (1990-2003)	Best-Track Years (2004-2014)
Gradient Wind (pos. root; cyclonic)	0.4171 (0.3958 to 0.4371)	0.4043 (0.3742 to 0.4327)	0.4620 (0.4330 to 0.4892)
Pure Rankine Vortex	0.3457 (0.3231 to 0.3672)	0.2751 (0.2422 to 0.3068)	0.4288 (0.3988 to 0.4571)
Modified Rankine Vortex (scaling parameter of 0.5)	0.6771 (0.6525 to 0.6803)	0.6036 (0.5804 to 0.6249)	0.7656 (0.7499 to 0.7795)
Cyclostrophic Wind	0.6799 (0.6657 to 0.6926)	0.6643 (0.6438 to 0.6829)	0.7555 (0.7392 to 0.7700)

Table 4: Correlation (explained variance, R^2; 95% confidence interval on R) Table between EBT IKE and PIKE that utilizes winds "found" at ROCI that were extracted from CCMP with EBT's knowledge on the parameter. Furthermore, EBT IKE is correlated with CCMP-IKE is shown in the last column. CCMP-IKE refers to Total CCMP-IKE (TCI).

Year(s)	EBT IKE vs. PIKE	EBT IKE vs. Resolved CCMP-IKE
2004	0.7760 (0.6022; 0.7307 to 0.8137)	0.6897 (0.4759; 0.5967 to 0.7636)
2005	0.6498 (0.4222; 0.5960 to 0.6969)	0.7792 (0.6072; 0.7179 to 0.8278)
2006	0.8870 (0.7868; 0.8535 to 0.9127)	0.8731 (0.7623; 0.8141 to 0.9138)
2007	0.7241 (0.5243; 0.6352 to 0.7933)	0.6753 (0.4560; 0.4858 to 0.8035)
2008	0.7652 (0.5855; 0.7166 to 0.8056)	0.7173 (0.5145; 0.6364 to 0.7818)
2009	0.8530 (0.7276; 0.7918 to 0.8967)	0.8119 (0.6592; 0.6836 to 0.8910)
2010	0.9294 (0.8638; 0.9131 to 0.9423)	0.9486 (0.8998; 0.9314 to 0.9613)
2011	0.8124 (0.6600; 0.7725 to 0.8452)	0.8680 (0.7534; 0.8269 to 0.8993)
2004-2011	0.8040 (0.6464; 0.7888 to 0.8174)	0.8403 (0.7061; 0.8215 to 0.8566)

Table 5: Descriptive values on the distribution for CCMP ROCI winds for the years 2004-2011. Every value is in SI units m s^{-1}. The last row is an average of the above column vector for each respective cell, and has been named the Climatological Average of the winds at ROCI.

Year	Minimum	25th percentile	Median	75th Percentile	Maximum
2004	4.4	8.1	9.7	11.6	19.4
2005	2.2	8.1	9.2	10.5	18.0
2006	5.1	7.5	8.8	10.3	17.2
2007	3.6	7.6	9.1	10.4	13.7
2008	3.5	7.6	8.9	10.0	14.3
2009	4.4	8.6	10.2	11.9	14.7
2010	3.2	7.8	9.0	10.4	17.9
2011	2.8	7.4	9.0	10.5	17.0
Climatological Average	3.7	7.8	9.2	10.7	16.5

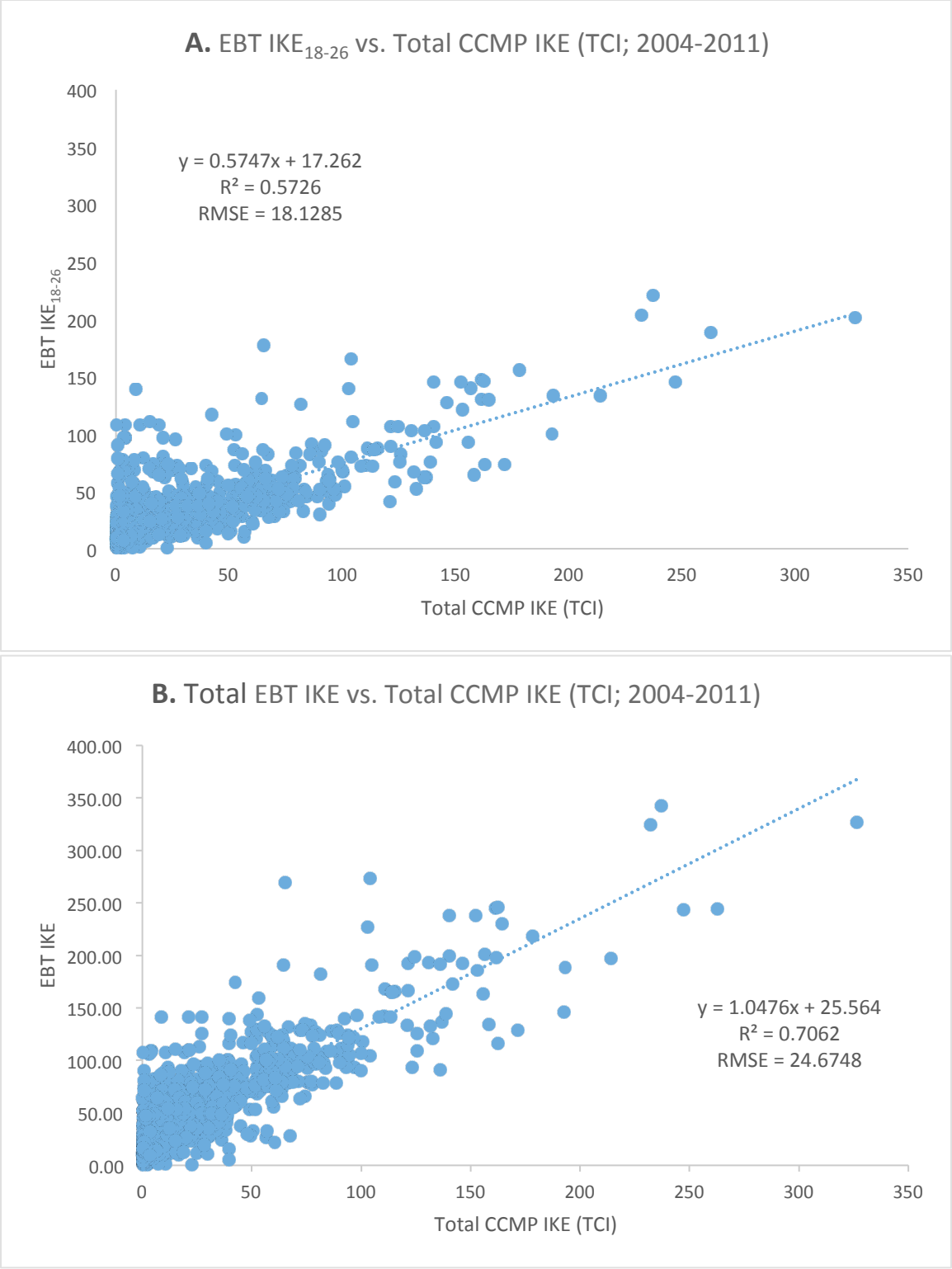

Figure 1: Scatter of IKE (in Terra Joules; TJ) from Cross-Calibrated Multi-Platform (CCMP) surface wind analysis (Atlas et al. 2011) with corresponding EBT data (Demuth et al. 2006) for Atlantic TCs from 2004-2011. Top (a) scatter shows the spread of EBT $IKE_{18\text{-}26}$ versus the resolved Total CCMP IKE (TCI). (b) Scatter of EBT (total) IKE versus Resolved TCI.

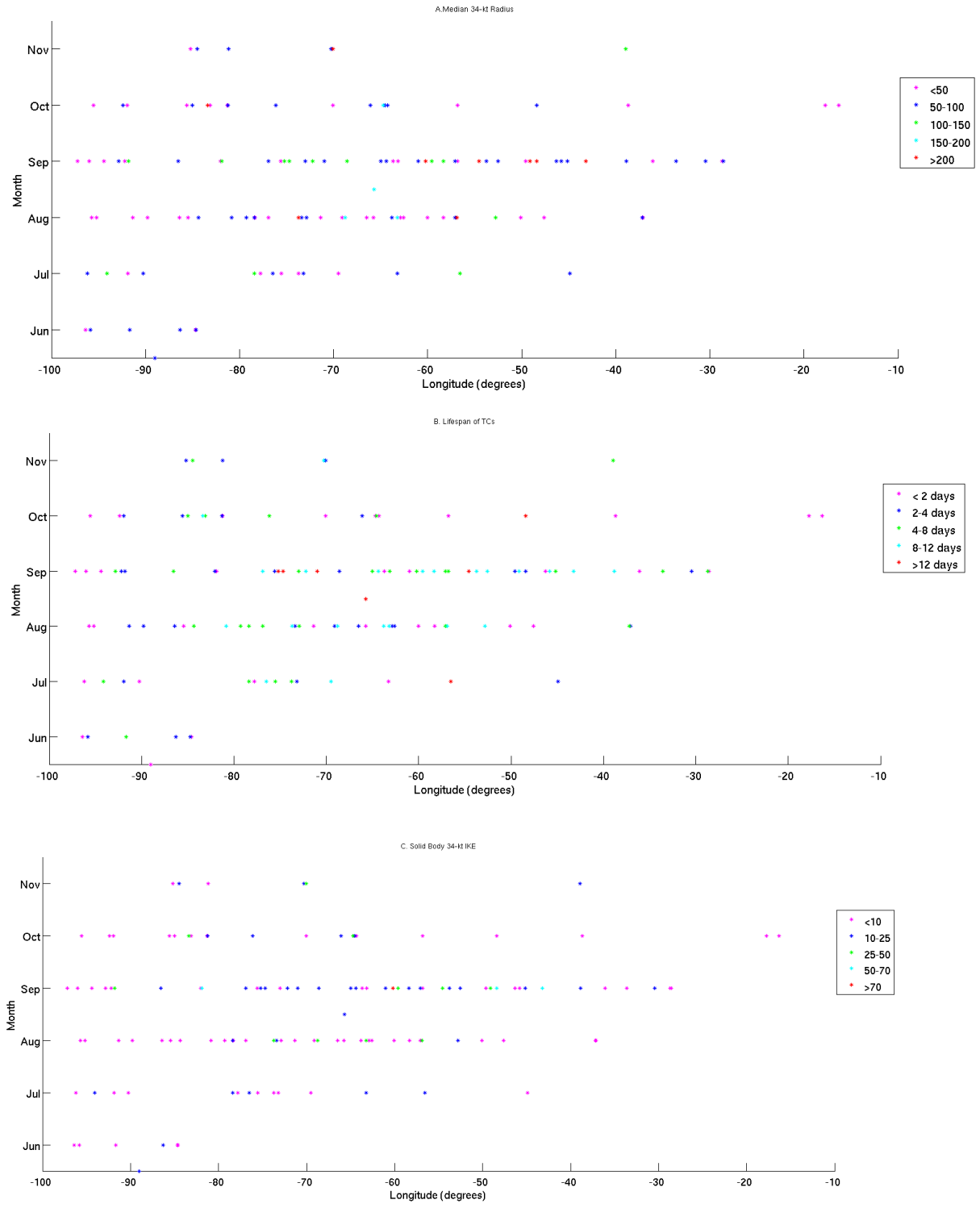

Figure 2: Scatterplot showing the month and longitude for all named TCs in the EBT dataset for the Tropical North Atlantic basin for the period 2004-2011. TCs are color-coded based on (a) the median 34-kt radius defined over the life span of the TC in nautical miles, (b) the length of time over which IKE (in TJ) was computed (i.e., lifespan), and (c) the median value of IKE_{18-26} defined over the life span of the TC in unit TJ.

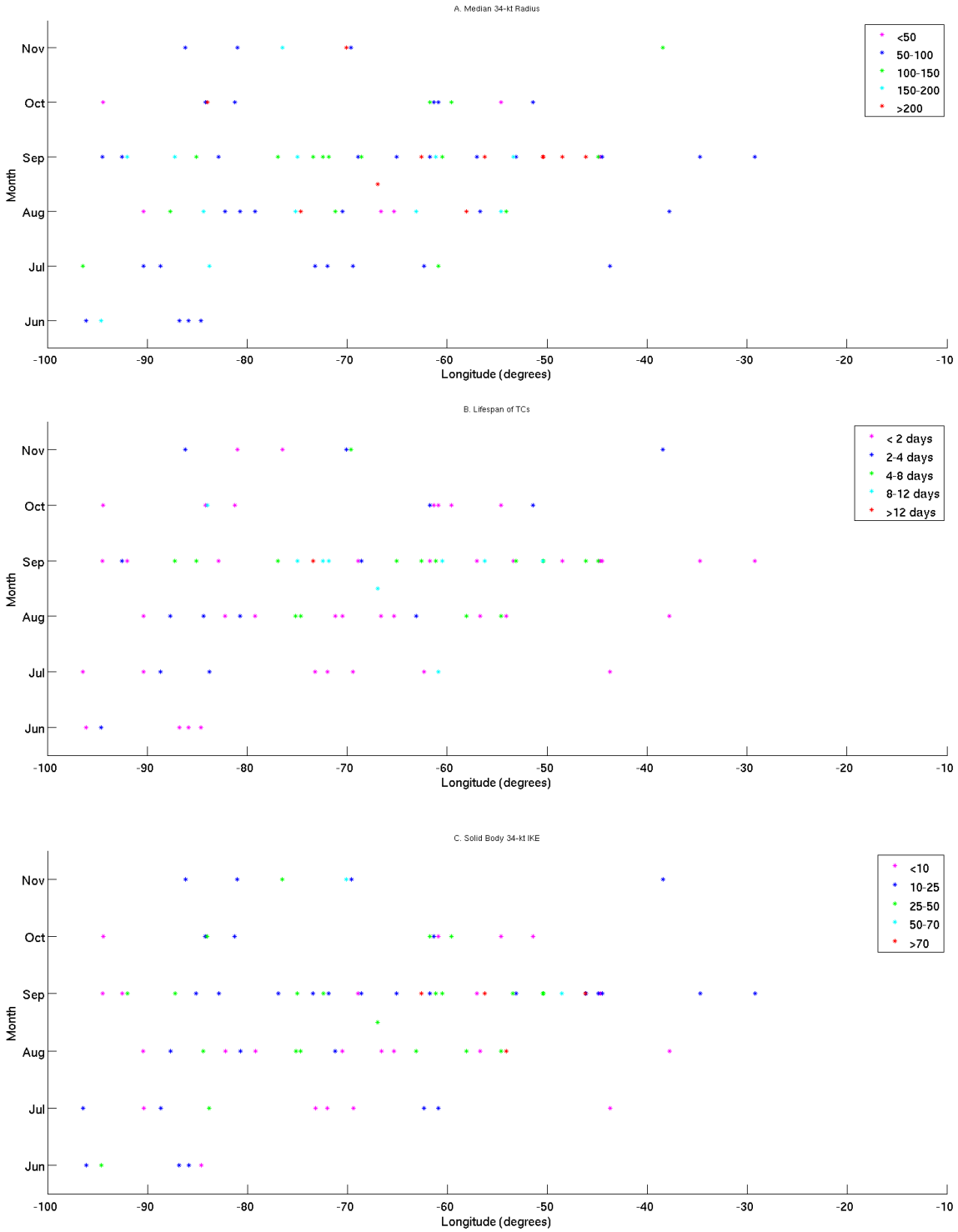

Figure 3: Same as Fig. 2 but derived from the resolved TCs with at least 34-kt winds from CCMP IKE, i.e., Total CCMP IKE (TCI; U ≥ 34-kt), in accordance to EBT data.

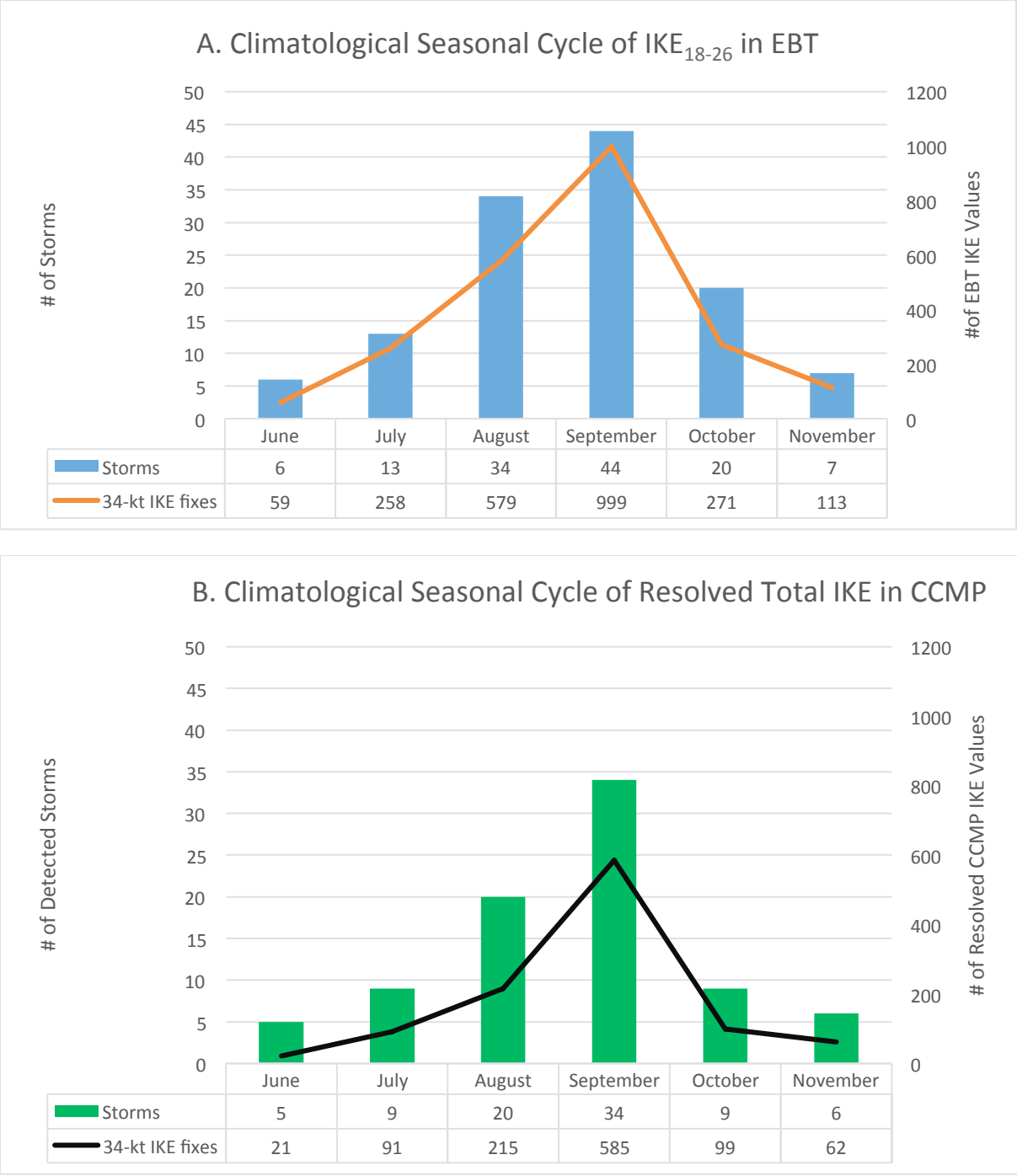

Figure 4: Climatological seasonal cycle of IKE (TJ) and number of North Atlantic TC's in a) EBT and b) CCMP dataset for the period 2004-2011.

a

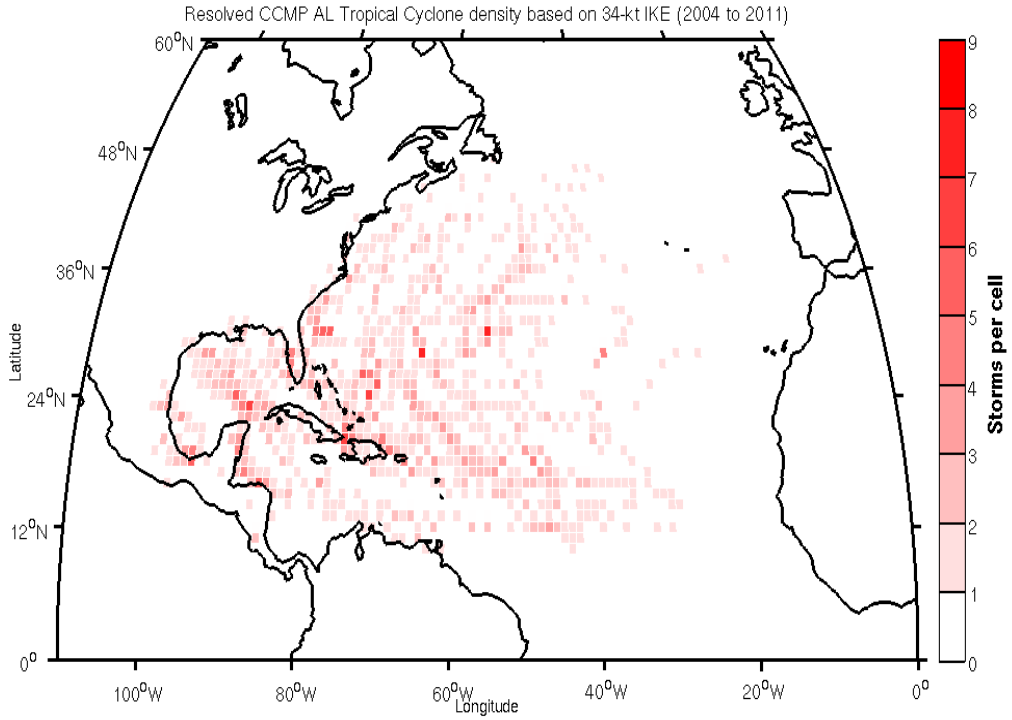

b

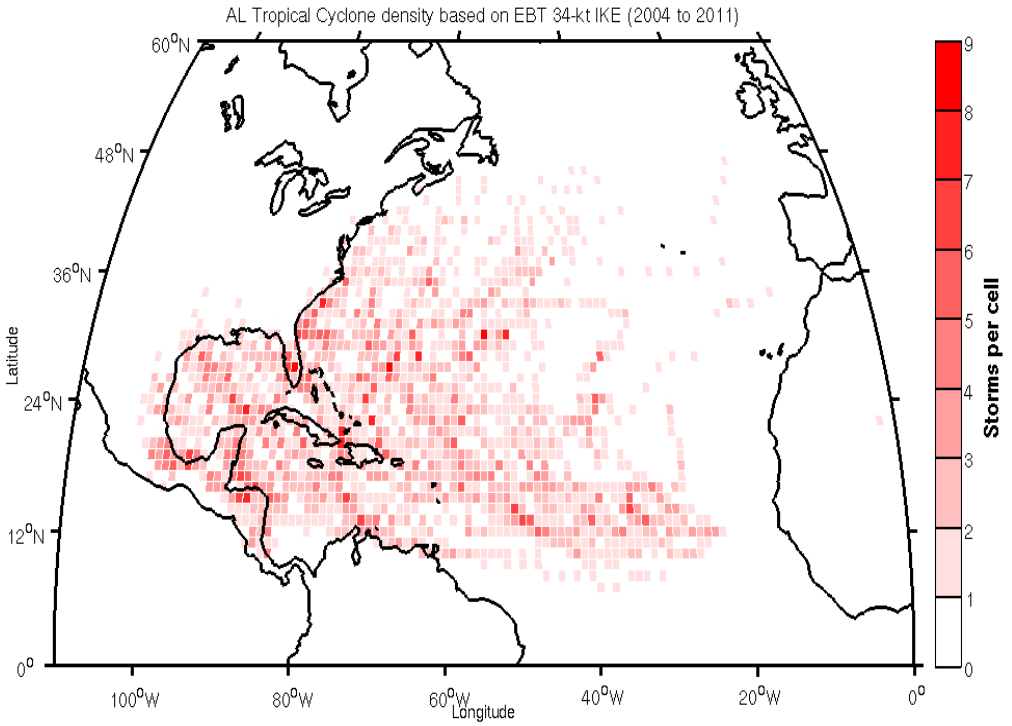

Figure 5: The composite track density (number of TCs with at least 34-kt winds per 1°x1° cell; see text for details) plot of North Atlantic TCs for the years 2004-2011 from a) CCMP and b) EBT data.

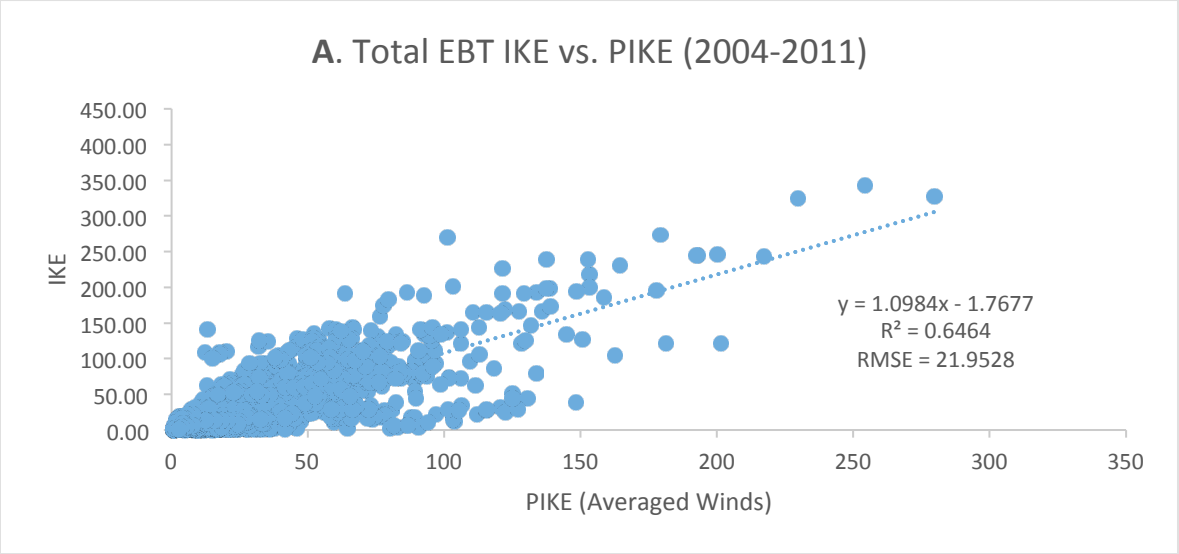

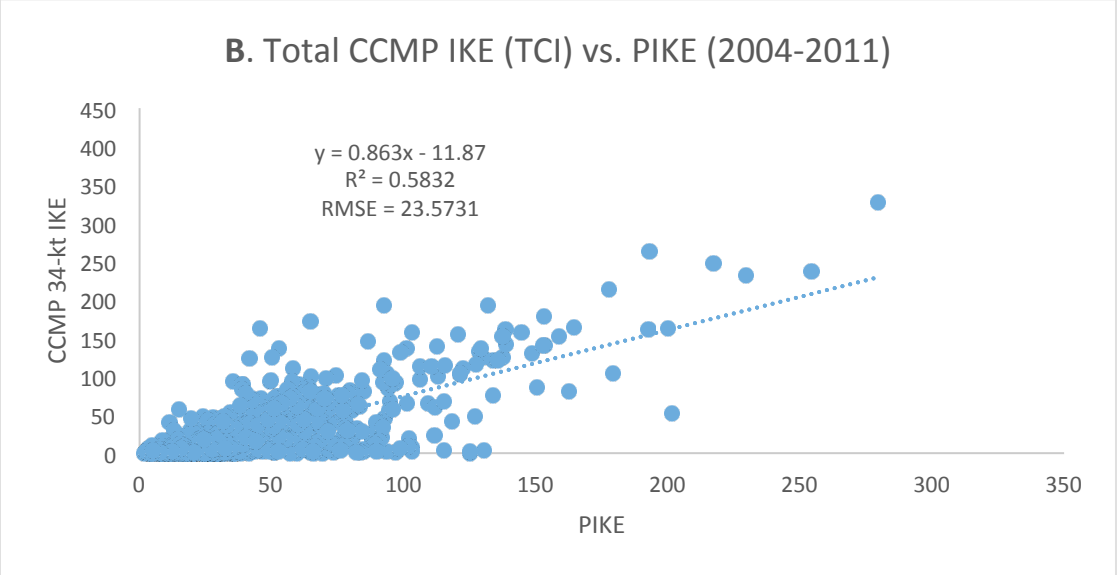

Figure 6: The scatter between: a) PIKE based on surface winds from CCMP winds and Total EBT IKE; b) Total CCMP IKE (TCI) and PIKE.

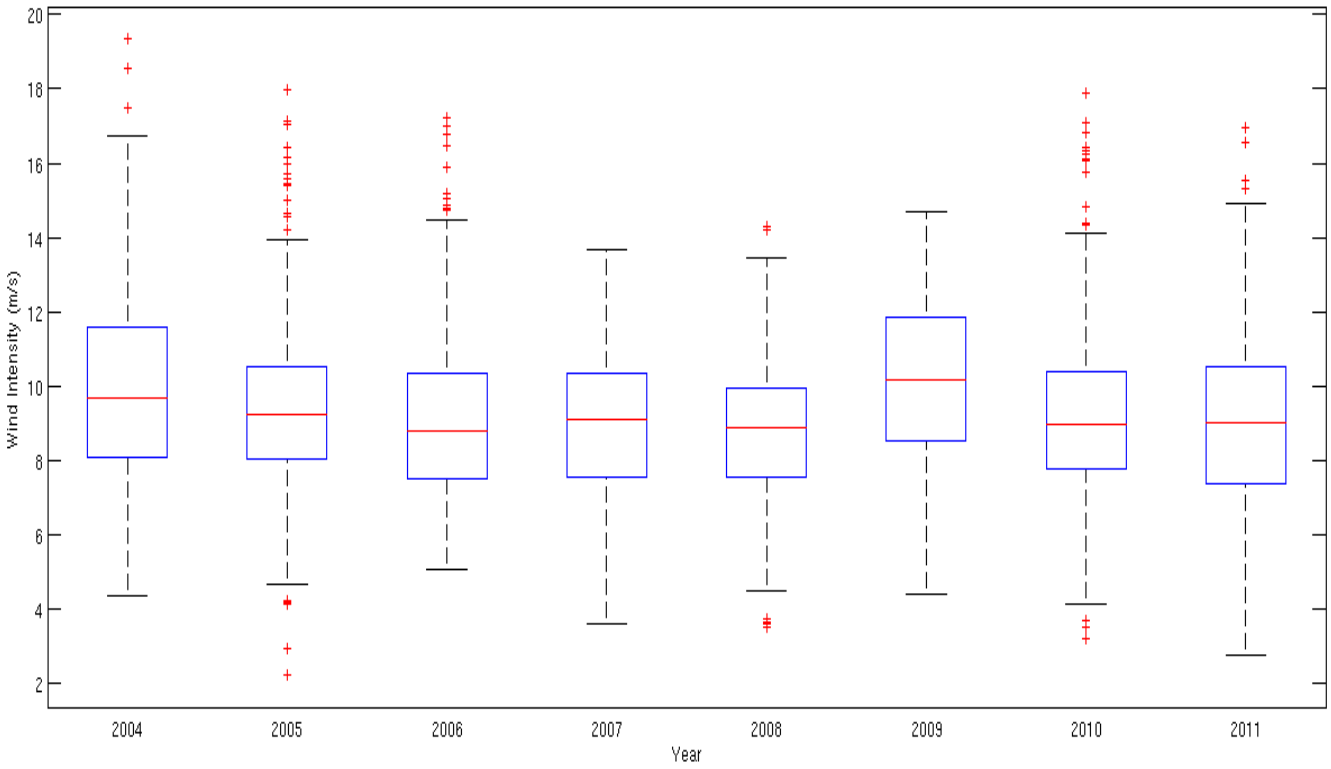

Figure 7: Boxplot depicting the distribution of the magnitude of the wind speed found at ROCI in CCMP based on EBT data.

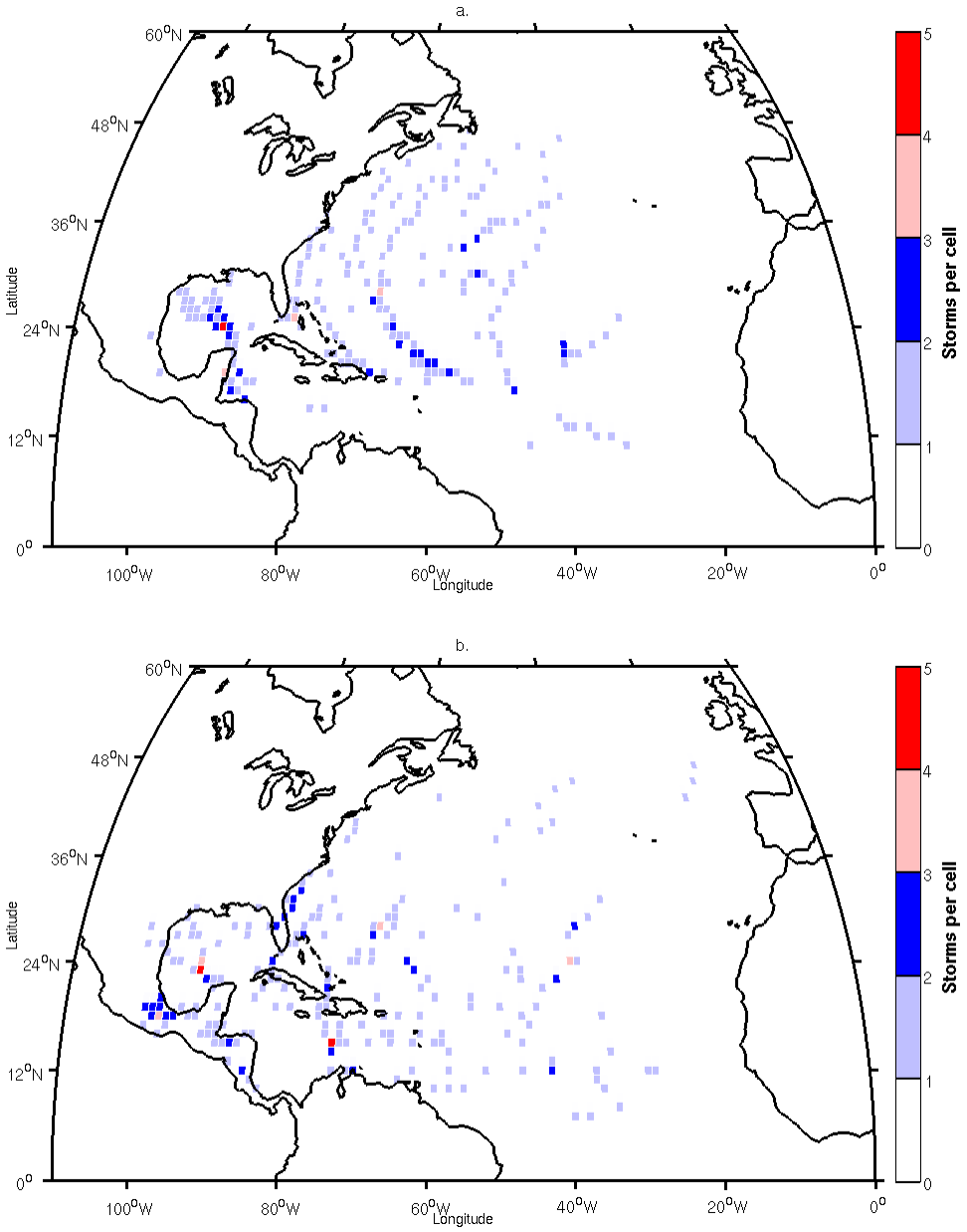

Figure 8: The composite track density plot of TCs for which the PIKE from CCMP validates most a) poorly and b) closely with EBT for the 2543 fixes between the years 2004-2011.